Optics Letters

Active modulation of intracavity laser intensity with the Pound–Drever–Hall locking for photoacoustic spectroscopy

Zhen Wang,[1] Haoyun Wei,[2] Yan Li,[2] Ruifeng Kan,[3] and Wei Ren[1,*]

[1] Department of Mechanical and Automation Engineering, and Shenzhen Research Institute, The Chinese University of Hong Kong, New Territories, Hong Kong SAR, China
[2] The State Key Laboratory of Precision Measurement Technology & Instruments, Department of Precision Instruments, Tsinghua University, Beijing 100084, China
[3] State Key Laboratory of Applied Optics, Changchun Institute of Optics, Fine Mechanics and Physics, Chinese Academy of Sciences, Changchun 130033, China
*Corresponding author: renwei@mae.cuhk.edu.hk

Received 23 December 2019; revised 23 January 2020; accepted 25 January 2020; posted 27 January 2020 (Doc. ID 386523); published 20 February 2020

Here we report a novel, to the best of our knowledge, method of active intracavity intensity modulation for cavity-enhanced photoacoustic spectroscopy (PAS) without the need for any external optical modulators. Based on the Pound–Drever–Hall (PDH) locking technique, a dither is added to the PDH error signal to periodically vary the locking point between the laser frequency and optical cavity within a sub-MHz frequency range. While significantly enhancing the intracavity laser intensity, the optical cavity also acts as an intensity modulator. As a proof-of-principle, we demonstrated the PAS of C_2H_2 by placing a photoacoustic cell (Q-factor ~ 10) inside a Fabry–Perot cavity (finesse ~ 628) and adopting the proposed intracavity intensity modulation scheme. By detecting the weak C_2H_2 line at 6412.73 cm^{-1}, the sensor achieves a normalized noise equivalent absorption (NNEA) coefficient of 1.5×10^{-11} $cm^{-1}WHz^{-1/2}$. This method enables the continuous locking of laser frequency and optical cavity, and it achieves the intracavity intensity modulation with an adjustable modulation depth as well.

https://doi.org/10.1364/OL.386523

Photoacoustic spectroscopy (PAS) is one of the most widely used optical sensing techniques for trace gases due to its high sensitivity and selectivity [1,2]. PAS relies upon the detection of the acoustic wave generated by the non-radiative relaxation process of the excited molecules. The generated acoustic wave is normally detected by different kinds of acoustic transducers such as microphone [3], quartz tuning fork [4–6], and microcantilever beam [7].

It is well known that the amplitude of the photoacoustic signal is directly proportional to the incident laser power. Any method that can be used to enhance optical power is attractive in PAS. In particular, cavity-enhanced PAS plays an important role in advancing photoacoustic gas detection to an ultrasensitive level. In this technique, the intracavity laser intensity is boosted in an optical cavity inside which an acoustic transducer is also placed. The key point for cavity-enhanced PAS is to achieve resonance between the optical cavity and laser frequency. The modulation technique such as Pound–Drever–Hall (PDH) and the optical feedback technique have been developed to lock the laser with optical cavity, which are commonly used in cavity-enhanced absorption spectroscopy [8–11], another spectroscopic technique that uses the high-finesse cavity to increase the effective path length. These locking techniques are also applicable in PAS to make use of the high intracavity intensity instead of the long optical path. It should be noted that the photoacoustic effect must be produced by periodically modulating the laser intensity or wavelength.

Several groups have recently reported cavity-enhanced photoacoustic sensors with significantly improved detection sensitivity that is evaluated by the normalized noise equivalent absorption (NNEA) coefficient. Note that NNEA is a key parameter to evaluate the sensitivity of different types of gas sensors by normalizing the incident laser power, absorption line-strength, and detection bandwidth. Hippler *et al.* [12] developed a cavity-enhanced H_2O sensor with a NNEA of 2.6×10^{-11} cm^{-1} $WHz^{-1/2}$ using the optical feedback technique. Similarly, Hayden *et al.* [13] presented an intracavity quartz-enhanced PAS (I-QEPAS) sensor for CO and H_2O detection with NNEA of 2.8×10^{-9} cm^{-1} $WHz^{-1/2}$ and 7×10^{-11} cm^{-1} $WHz^{-1/2}$, respectively. The optical feedback locking method was employed to couple a quantum cascade laser with a linear Brewster window cavity. Borri *et al.* [14] demonstrated I-QEPAS by detecting CO_2 at 4.33 μm using a quartz tuning fork inside a bow-tie cavity, and the authors achieved a NNEA of 3.2×10^{-10} cm^{-1} $WHz^{-1/2}$. All these studies adopted the intensity modulation strategy by modulating the laser current to make the laser frequency in resonance with the cavity periodically.

Recently we have demonstrated an ultrasensitive photoacoustic sensor with a NNEA of 1.1×10^{-11} cm^{-1} $WHz^{-1/2}$ by employing a high-finesse (> 9000) optical cavity with the PDH technique [15]. The optical intensity modulation was achieved by using a fiber-coupled optical switch. Pan *et al.* [16] reported a similar sensor using the PDH method, and the intensity modulation was performed with a fiber-coupled $LiNbO_3$ intensity modulator. However, these expensive external modulators can only be used in a limited wavelength range, and the use of optical modulators may interrupt the laser-cavity locking status.

In this Letter, we proposed a new intensity modulation strategy for intracavity PAS without using any external optical modulators. A dither signal is added to the standard PDH error signal so that the locking point is adjusted periodically and finely. This strategy controls the relative difference between the laser frequency and cavity mode down to sub-MHz, thus leading to the active modulation of intracavity laser intensity. As a result, we enable a continuous locking of laser and cavity with an adjustable modulation depth, which simplifies the sensing system and improves the system stability. As a proof-of-principle, the proposed modulation scheme is adopted in a cavity-enhanced photoacoustic sensor for C_2H_2 detection.

Figure 1 depicts the schematic of cavity-enhanced PAS with the active intracavity intensity modulation. The narrow linewidth (0.1 kHz) fiber laser (NKT Photonics, E15) could be tuned from 1559.33 nm to 1560.4 nm. The laser was fiber connected to an electro-optic modulator (EOM, Thorlabs LN65S-FC) that modulated the laser radiation at 20 MHz to generate two sidebands for PDH locking. The laser output was collimated and transmitted through two convex lenses (L1, $f = 30$ mm; and L2, $f = 50$ mm) to achieve the appropriate mode matching with the fundamental Gaussian mode of the optical cavity. The Fabry–Perot (F-P) cavity used in this work consists of two plano-concave mirrors (Layertec Inc.) with a reflectivity of 99.5%, corresponding to a finesse of 628. Both mirrors have the same radius of curvature of 150 mm and are separated by 80 mm. One of the mirrors was attached to a PZT so that the cavity length could be finely tuned.

The conventional stainless-steel photoacoustic cell placed inside the F-P cavity consists of a cylindrical resonator and two buffer volumes. The acoustic resonator was designed to have a diameter of 3 mm and a length of 35 mm. The two buffer volumes with a diameter of 12 mm and length of 17.5 mm made on both ends of the acoustic resonator mitigate the external noise and "window signal". An electret microphone (Knowles Electronics, US; sensitivity 31.6 mV/Pa) was mounted in the middle of the resonator for acoustic detection. After being amplified by a low-noise preamplifier (Stanford Research, SR560), the electrical signal was demodulated by a lock-in amplifier with a detection bandwidth of 10 Hz. The photoacoustic cell operating at its first longitudinal mode was characterized to have a resonant frequency (f_0) of 3.32 kHz and Q-factor of 10 at the atmospheric pressure. Both the F-P cavity and photoacoustic cell were enclosed in a stainless-steel vacuum chamber with two ports used for gas sampling and two CaF_2 windows for optical access.

To implement the PDH technique with a simplified optical setup, we utilized the transmitted light through the cavity for the locking purpose instead of the cavity reflection signal [15]. As illustrated in Fig. 1, the cavity transmission was detected by a photodetector (bandwidth 150 MHz) and further processed by a PDH phase demodulator (Toptica, PDD110). The generated error signal was used by a laser servo (Toptica, Facl110) to realize the laser-cavity locking by actively controlling the cavity length.

Although the optical configuration is similar to the conventional cavity-enhanced PAS, we proposed, to the best of our knowledge, a new method of making use of the optical cavity directly as an intensity modulator. The optical cavity has equidistant longitudinal modes separated by the free spectral range (FSR). The incident laser has a maximum transmission when the laser frequency matches one of the cavity modes. Here each cavity mode features a Lorentzian profile with a full width at half maximum (FWHM) of 2.8 MHz only. The cavity transmission varies dramatically when the cavity mode scans across the laser frequency. Hence, the cavity mode acts as an active modulator with a modulation depth from 0% to nearly 100% if one can

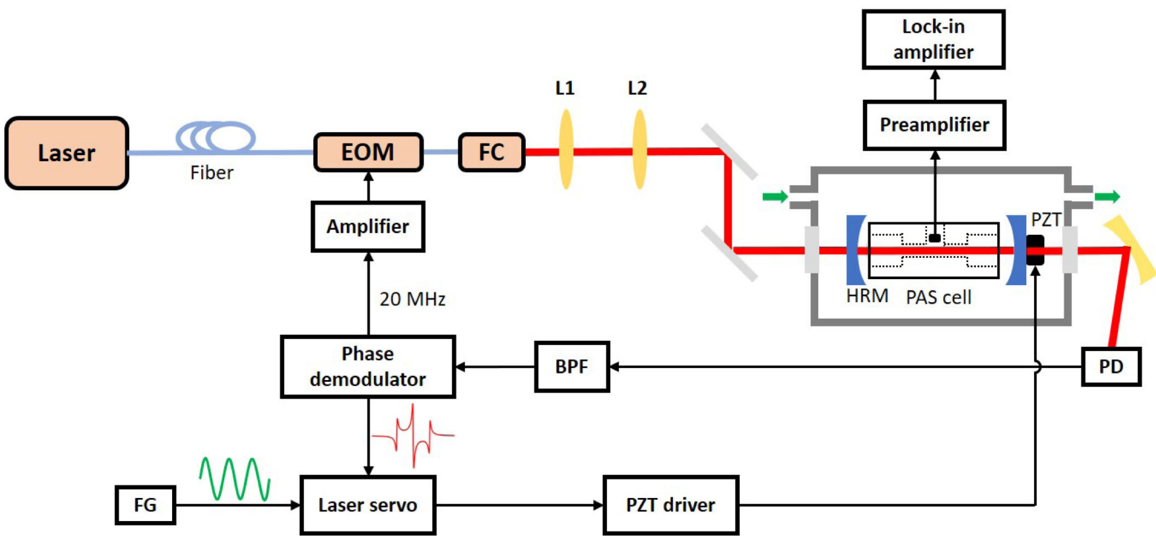

Fig. 1. Schematic of cavity-enhanced PAS with the active intracavity intensity modulation. FG, function generator; EOM, electro-optic modulator; FC, fiber collimator; PD, photodetector; BPF, band-pass filter; HRM, high-reflectivity mirror.

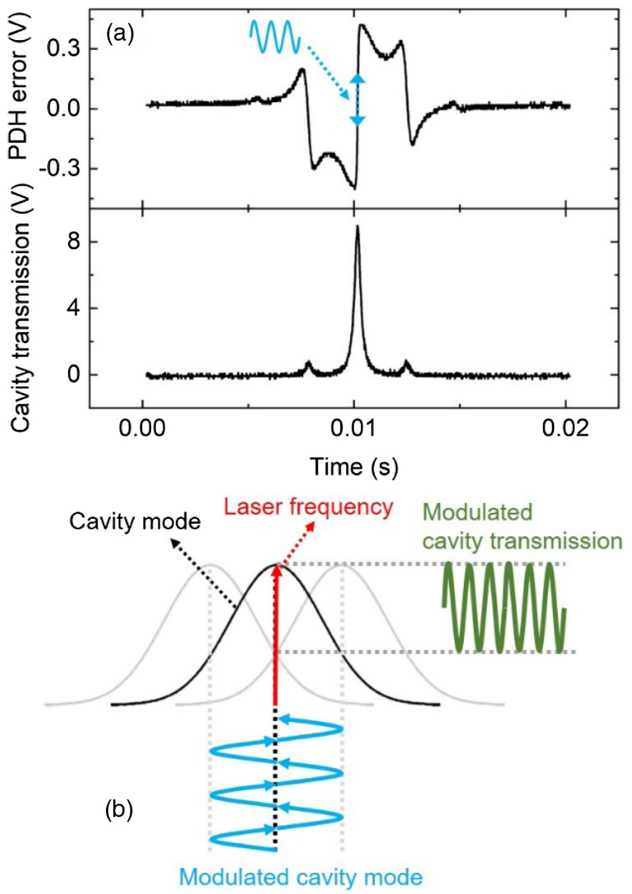

Fig. 2. (a) Typical cavity transmission (bottom panel) and PDH error signal (top panel) measured by scanning the cavity mode across the laser frequency. The modulation of the locking point indicated by the blue arrow shown in the PDH error signal determines the relative position between the laser frequency and cavity mode; (b) principle of the PDH locking with active intensity modulation.

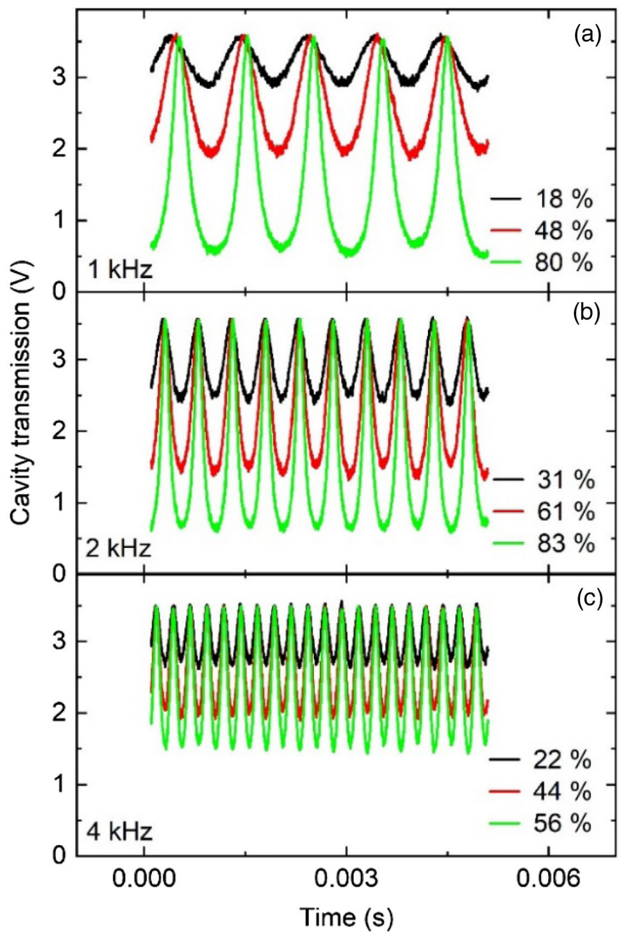

Fig. 3. Representative intensity modulation at different modulation depths and modulation frequencies: (a) 1 kHz, (b) 2 kHz, and (c) 4 kHz.

periodically control the relative position between the laser frequency and cavity mode. However, it is difficult to achieve such a precise control by simply tuning the laser wavelength or cavity length due to the very narrow FWHM of the cavity mode.

PDH locking is a powerful technique of maintaining the resonant condition. Figure 2(a) presents the typical PDH error signal and cavity transmission obtained in this work when the cavity mode scans across the laser frequency by tuning the cavity length. As illustrated in the top panel of Fig. 2(a), the antisymmetric error signal has a steep slope crossing zero, which stands for the resonant condition and maximum cavity transmission. If an extra dither signal is added to the PDH error signal, the locking point crosses zero periodically that generates an actively controlled cavity transmission. The working principle is shown in Fig. 2(b). As the cavity mode is a symmetric profile, the dither signal at frequency $f_0/2$ generates an intensity modulation at frequency f_0. Additionally, the modulation depth could be varied by changing the amplitude of the dither.

Figure 3 illustrates the representative signals of cavity transmission that directly reflect the intracavity intensity modulation. We investigated the intensity modulation at different modulation frequencies and modulation depths (i.e., 1 kHz, 18%–80%; 2 kHz, 31%–83%; and 4 kHz, 22%–56%). Our technique locks the laser frequency with the optical cavity at a time-varying locking point to generate the active intracavity intensity modulation. Such a continuous locking is always maintained during the entire modulation process compared to the previous work that the current modulation or external modulator (i.e., optical switch) would interrupt the locking status [14,15]. Note that the current system has a larger noise and relatively limited modulation depth at the higher modulation frequency of 4 kHz, which is mainly caused by the limited bandwidth of the PZT.

The narrow-linewidth fiber laser used in this work could be tuned across an absorption line of C_2H_2 centered at $6412.73\ cm^{-1}$. The calculated absorption coefficient of 1% C_2H_2 is depicted in Fig. 4(a) based on the HITRAN database [17], showing a peak value of $\sim 10^{-5}\ cm^{-1}$. We used this weak C_2H_2 line to demonstrate the proof-of-principle for cavity-enhanced PAS. Figure 4(b) shows the representative intracavity photoacoustic signals of 1% C_2H_2/N_2 at 1 atm for three different modulation depths along with Voigt fitting. The measurement time of each data point is ~ 0.4 s, and the total duration of a wavelength scan is ~ 120 s, which is limited by the temperature-tuning speed of the fiber laser. Note that the constant background offset was subtracted from the signal. The modulation frequency of the dither was selected to be 1.66 kHz so that the generated acoustic signal has the same resonance

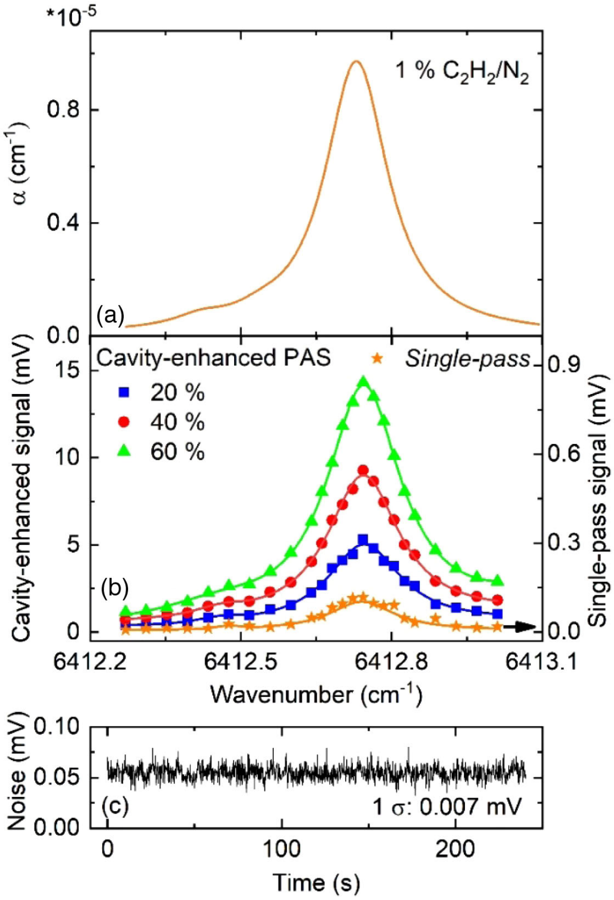

Fig. 4. (a) Calculated absorption coefficient of 1% C_2H_2/N_2 based on the high-resolution transmission molecular absorption database; (b) representative cavity-enhanced photoacoustic spectra at different modulation depths (20%, 40%, and 60%) and the single-pass photoacoustic spectrum of 1% C_2H_2/N_2 at 1 atm along with the Voigt fitting; (c) background noise.

frequency of the photoacoustic cell. With the modulation depth increased from 20% to 60%, the peak of the photoacoustic signal increases from 5.4 mV to 14.35 mV. Besides the target line at 6412.73 cm^{-1}, another weaker C_2H_2 line centered at 6412.42 cm^{-1} is also distinguishable using the current system.

Comparing with the conventional PAS without the cavity enhancement, we removed the optical cavity and added an optical switch for the purpose of intensity modulation. The measured single-pass photoacoustic signal is also plotted in Fig. 4(b) for comparison, showing a much smaller amplitude of 0.11 mV due to the low incident-laser intensity.

Finally, the system noise was measured for 240 s by filling the gas cell with ambient air and fixing the laser wavelength at the selected absorption line at the modulation depth of 60%. As shown in Fig. 4(c), the background noise has an offset of 0.06 mV and a 1-σ deviation of 0.007 mV. Considering the detection signal-to-noise ratio and the absorption coefficient of C_2H_2 at this specific wavelength, the current system leads to a NNEA coefficient of 1.5×10^{-11} cm^{-1} $WHz^{-1/2}$, which is comparable with state-of-the-art cavity-enhanced PAS [15].

In conclusion, we report, to the best of our knowledge, a new strategy of intracavity intensity modulation for cavity-enhanced PAS. Without using any external optical modulators, a dither is added to the PDH error signal so that the locking point between the laser and the optical cavity could be actively controlled. In particular, the cavity mode is finely modulated across the laser frequency within sub-MHz so that the optical cavity itself acts as an intensity modulator. The intensity modulation depth could be adjusted over a wide range by adjusting the dither amplitude if the modulation frequency is selected within the bandwidth of the PDH system. By detecting a weak C_2H_2 line at 6412.73 cm^{-1} in a photoacoustic cell (Q-factor ~ 10) that was placed inside a F-P cavity (finesse 628), we achieved a NNEA coefficient of 1.5×10^{-11} cm^{-1} $WHz^{-1/2}$ using the proposed intracavity intensity modulation scheme. In the future, we plan to extend this method to mid-infrared gas sensor development with quantum cascade lasers that access the much stronger footprint spectra of many molecules [18,19].

Funding. National Natural Science Foundation of China (51776179); Research Grants Council, University Grants Committee (14206317); Open Research Fund from the State Key Laboratory of Applied Optics (SKLAO-201901).

Disclosures. The authors declare no conflicts of interest.

REFERENCES

1. A. Miklós, P. Hess, and Z. Bozóki, Rev. Sci. Instrum. **72**, 1937 (2001).
2. M. W. Sigrist, Rev. Sci. Instrum. **74**, 486 (2003).
3. B. A. Paldus, T. G. Spence, R. N. Zare, J. Oomens, F. J. M. Harren, D. H. Parker, C. Gmachl, F. Cappasso, D. L. Sivco, J. N. Baillargeon, A. L. Hutchinson, and A. Y. Cho, Opt. Lett. **24**, 178 (1999).
4. A. A. Kosterev, Y. A. Bakhirkin, R. F. Curl, and F. K. Tittel, Opt. Lett. **27**, 1902 (2002).
5. H. Wu, L. Dong, H. Zheng, Y. Yu, W. Ma, L. Zhang, W. Yin, L. Xiao, S. Jia, and F. K. Tittel, Nat. Commun. **8**, 1 (2017).
6. L. Dong, A. A. Kosterev, D. Thomazy, and F. K. Tittel, Appl. Phys. B **100**, 627 (2010).
7. J. Peltola, M. Vainio, T. Hieta, J. Uotila, S. Sinisalo, M. Metsälä, M. Siltanen, and L. Halonen, Opt. Express **21**, 10240 (2013).
8. R. W. P. Drever, J. L. Hall, F. V. Kowalski, J. Hough, G. M. Ford, A. J. Munley, and H. Ward, Appl. Phys. B **31**, 97 (1983).
9. E. D. Black, Am. J. Phys. **69**, 79 (2001).
10. A. G. V. Bergin, G. Hancock, G. A. D. Ritchie, and D. Weidmann, Opt. Lett. **38**, 2475 (2013).
11. L.-S. Ma, J. Ye, P. Dubé, and J. L. Hall, J. Opt. Soc. Am. B **16**, 2255 (1999).
12. M. Hippler, C. Mohr, K. A. Keen, and E. D. McNaghten, J. Chem. Phys. **133**, 044308 (2010).
13. J. Hayden, B. Baumgartner, J. P. Waclawek, and B. Lendl, Appl. Phys. B **125**, 159 (2019).
14. S. Borri, P. Patimisco, I. Galli, D. Mazzotti, G. Giusfredi, N. Akikusa, M. Yamanishi, G. Scamarcio, P. De Natale, and V. Spagnolo, Appl. Phys. Lett. **104**, 091114 (2014).
15. Z. Wang, Q. Wang, W. Zhang, H. Wei, Y. Li, and W. Ren, Opt. Lett. **44**, 1924 (2019).
16. Y. Pan, L. Dong, H. Wu, W. Ma, L. Zhang, W. Yin, L. Xiao, S. Jia, and F. K. Tittel, Atmos. Meas. Tech. **12**, 1905 (2019).
17. HITRANonline, "The HITRAN Database," https://hitran.org/.
18. S. Borri, G. Insero, G. Santambrogio, D. Mazzotti, F. Cappelli, I. Galli, G. Galzerano, M. Marangoni, P. Laporta, V. Di Sarno, L. Santamaria, P. Maddaloni, and P. De Natale, Appl. Phys. B **125**, 18 (2019).
19. S. Bartalini, S. Borri, P. Cancio, A. Castrillo, I. Galli, G. Giusfredi, D. Mazzotti, L. Gianfrani, and P. De Natale, Phys. Rev. Lett. **104**, 083904 (2010).